

# Seismic Performance of Precast Segmental Bridge Superstructures with Internally Bonded Prestressing Tendons



**Sami Megally, Ph.D.**  
Assistant Project Scientist  
Department of Structural Engineering  
University of California at San Diego  
La Jolla, California



**Frieder Seible, Ph.D., P.E.**  
Executive Associate Dean and Professor  
Department of Structural Engineering  
University of California at San Diego  
La Jolla, California



**Manu Garg**  
Graduate Research Assistant  
Department of Structural Engineering  
University of California at San Diego  
La Jolla, California



**Robert K. Dowell, Ph.D., P.E.**  
Principal  
Dowell-Holombo Engineering, Inc.  
San Diego, California

---

*A research project is currently in progress to investigate the seismic performance of segment-to-segment joints of precast segmental concrete bridges. This paper presents the experimental and analytical results of two large-scale tests which model the superstructure response of a prototype precast segmental bridge, post-tensioned with internally bonded tendons, under fully reversed vertical cyclic displacements. The joints of the first test unit were epoxy bonded with no reinforcement crossing the joints other than the prestressing steel. The second test unit had a reinforced cast-in-place deck closure with the remaining portions of the joints connected by epoxy. Both test units were subjected to fully reversed cyclic loads simulating earthquake vertical motions. It was found that both test units could undergo significant seismic displacements, but their failure modes were considerably different. The paper also presents results from nonlinear finite element modeling of the simulated seismic response of the test units. The results showed that segment-to-segment joints could undergo significant repeated opening and closure before failure.*

---

**P**recast segmental concrete bridge construction is popular because of its well-known advantages of quality control and construction schedule over conventional cast-in-place construction. However, the popularity of precast segmental bridges is hampered in high seismic zones because of the lack of information on their seismic performance.

The AASHTO Guide Specification for Design and Construction of Segmental Concrete Bridges<sup>1</sup> permits the use of precast segmental construction in high seismic zones (Zones 3 and 4), provided that the precast segments are epoxy bonded. The same AASHTO Guide Specification<sup>1</sup> also requires that external tendons should achieve no more than 50 percent of the superstructure post-tensioning.

In other words, fully bonded internal tendons should achieve at least 50 percent of the post-tensioning. In addition to these requirements, precast segmental bridge construction without mild steel reinforcement crossing the segment-to-segment joints is not recommended in current practice in high seismic zones such as California.

The above-mentioned recommendations and restrictions of current practice are justified by the lack of information on seismic performance of precast segmental bridges. Thus, a comprehensive research project has been developed by ASBI (American Segmental Bridge Institute) and funded by Caltrans (California Department of Transportation) to investigate the seismic performance of precast segmental bridge superstructures.

In order to investigate the seismic performance of precast segmental bridges, a large-scale experimental research project is currently in progress at the University of California, San Diego (UCSD). This research project consists of the following three phases:

- **Phase I:** To investigate the seismic performance of segment-to-segment joints in superstructures with different ratios of internal to external post-tensioning under simulated fully reversed cyclic loading. In this first phase, only superstructure joints close to midspan in regions with high positive flexural moments and low shears are considered. Phase I consists of the following two parts:

- (1) **Phase I-A:** Superstructures with 100 percent internal post-tensioning (Test Units 100INT and 100INTCIP; see Table 1).

- (2) **Phase I-B:** Superstructures with 100 percent external post-tensioning and superstructures with 50 percent internal post-tensioning combined with 50 percent external post-

Table 1. Test matrix.

Phase	Test unit	Test description
I-A	100INT	100 percent internal post-tensioning
	100INTCIP	100 percent internal post-tensioning and cast-in-place deck closure joints
I-B	100EXT	100 percent external post-tensioning
	50INT/50EXT	50 percent internal + 50 percent external post-tensioning

tensioning (Test Units 100EXT and 50INT/50EXT, respectively). Test Units 100EXT and 50INT/50EXT are identical to Test Unit 100INT of Phase I-A with the only difference being the percentage of external post-tensioning. Test Unit 100EXT, with 100 percent external post-tensioning, does not satisfy the current requirement of the AASHTO Guide Specification<sup>1</sup> that no more than 50 percent of post-tensioning should be achieved by external tendons.

- **Phase II:** To investigate the seismic performance of superstructure joints close to the supports in regions with high shears and negative flexural moments.

- **Phase III:** To investigate the system performance of segmental superstructure and columns under longitudinal seismic loading.

The experimental program and the analytical model calibrations of the two tests from Phase I-A with 100 percent internally bonded tendons are presented in this paper. Each test unit consisted of six precast segments, which were epoxy bonded. The entire joint surfaces of the first test unit were epoxy bonded with no mild steel reinforcement crossing the joints, which did not conform to the current recommended practice in high seismic zones. The second test unit had a reinforced cast-in-place deck closure at the location of each joint, with the web and bottom soffit of the segments epoxy bonded.

The major objectives of this first phase of the research program are to investigate: (1) joint behavior in terms of opening and closure under repeated cyclic loads simulating earthquake effects, (2) development of crack patterns, and (3) modes of failure.

Three-dimensional finite element models of the test units were developed. The models took into account concrete cracking and crushing, opening and closure of segment-to-segment

joints and the inelastic characteristics of prestressed and non-prestressed steels. The finite element models were validated with the experimental results presented in this paper.

The calibrated analytical models are powerful tools for parametric and design studies that provide useful information, which may be difficult to obtain experimentally. They also provide a better understanding of the observed behavior of segment-to-segment joints.

The main objective of the analytical models described in this paper is to determine the major characteristics of joint behavior. The results will be used to develop a comprehensive global finite element model of bridge structures; this global model can be used for analytical parametric studies investigating different superstructure geometries, prestress levels, and seismic input variations.

## PROTOTYPE STRUCTURE

Test units of Phase I of this experimental program are based on the prototype structure shown in Fig. 1. The superstructure consists of three 100 ft (30.48 m) interior spans and 75 ft (22.86 m) exterior spans with a total length of 450 ft (137.16 m) and is prestressed with a harped shape tendon (see Fig. 1a).

Because of its short spans, the prototype structure is constructed using the span-by-span method. Fig. 1b shows the cross section of the prototype superstructure.

The prototype structure was designed according to the AASHTO Guide Specification for Design and Construction of Segmental Concrete Bridges,<sup>1</sup> the AASHTO-PCI-ASBI Segmental Box Girder Standards for Span-by-Span and Balanced Cantilever Construction<sup>2</sup> and the AASHTO Standard Specifications for Highway Bridges.<sup>3</sup>

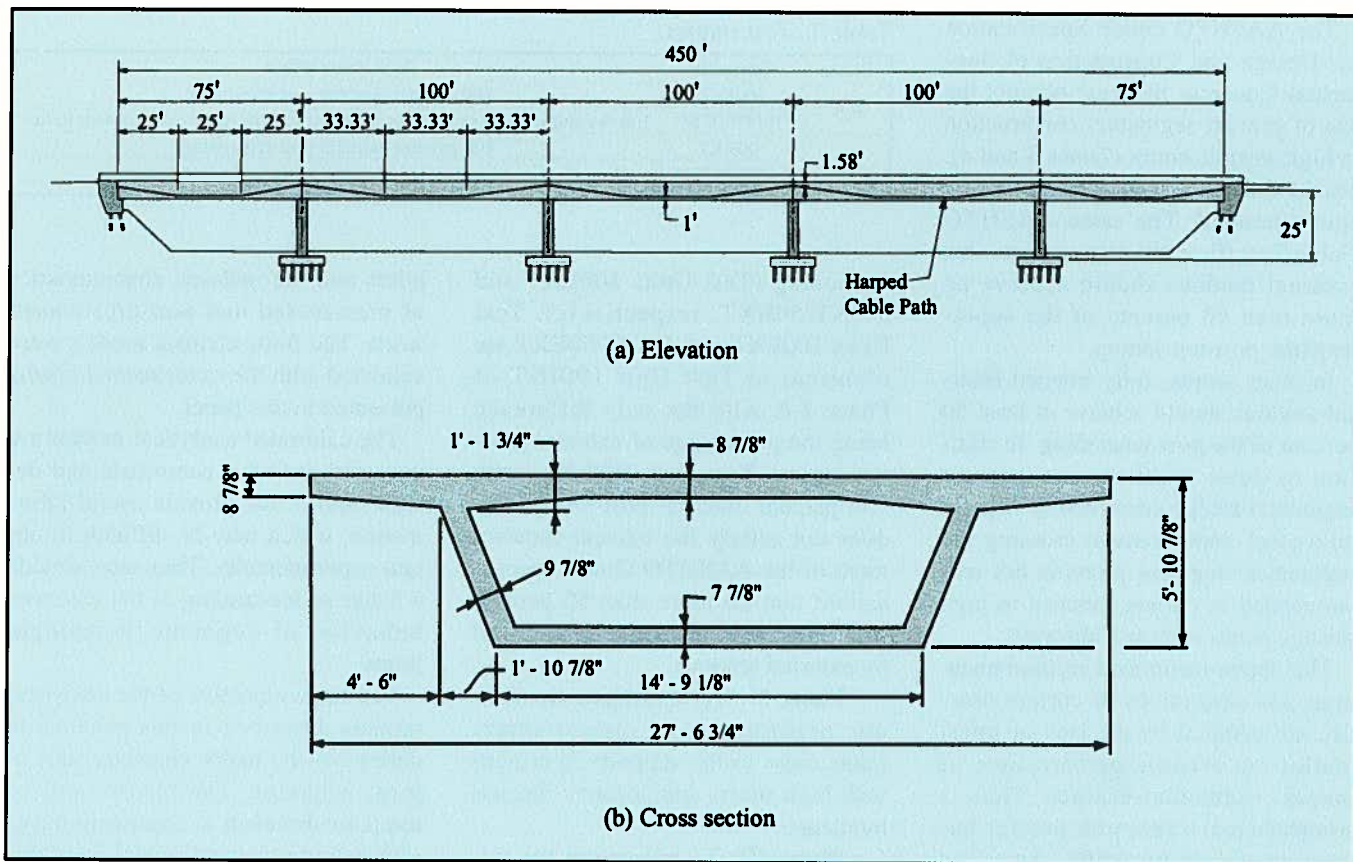


Fig. 1. Prototype structure: (a) Elevation; and (b) Cross section.

## EXPERIMENTAL PROGRAM

This section gives a description of the test units and their method of construction. The test setup and sequence of loading of the test units are also described in this section.

## Description of Test Units

The critical location of the prototype structure for positive bending under dead load and seismic forces was found to be approximately at midspan.<sup>4</sup> The test units model the

middle third of the prototype span in which the tendon is horizontal (see Fig. 1a). For the laboratory tests, they were designed at two-thirds scale of the prototype structure.

Fig. 2 shows a typical test unit, sim-

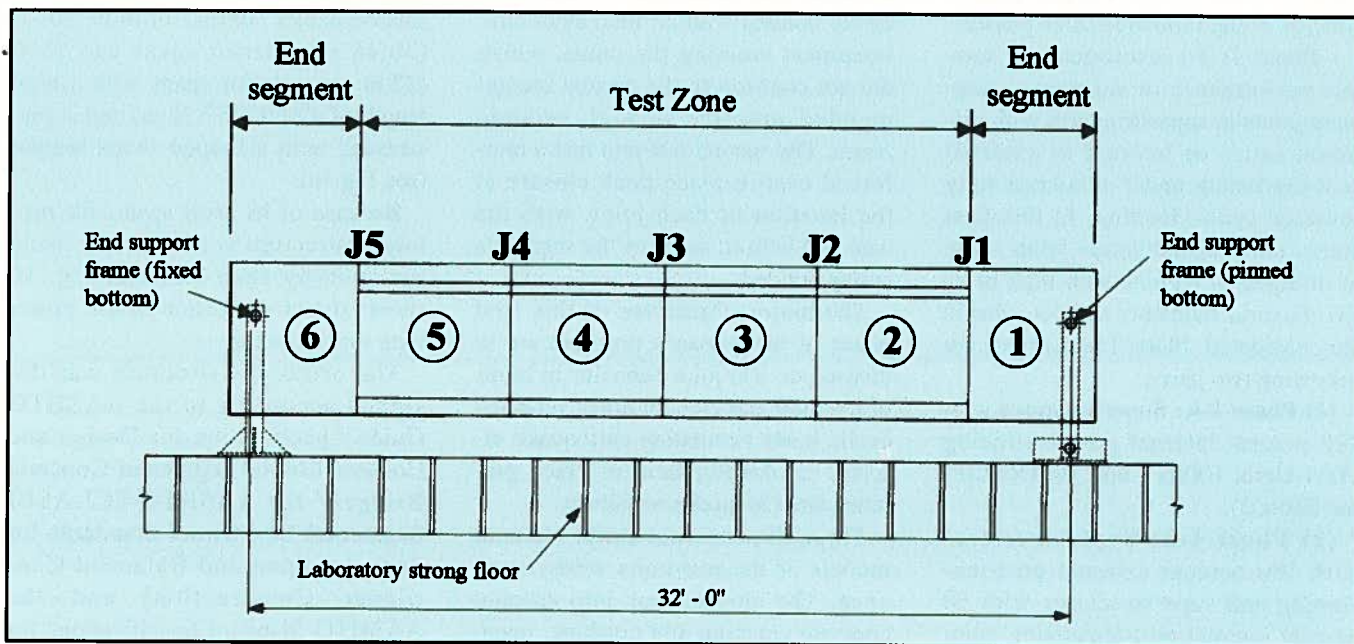


Fig. 2. Joint and segment numbering of test units.

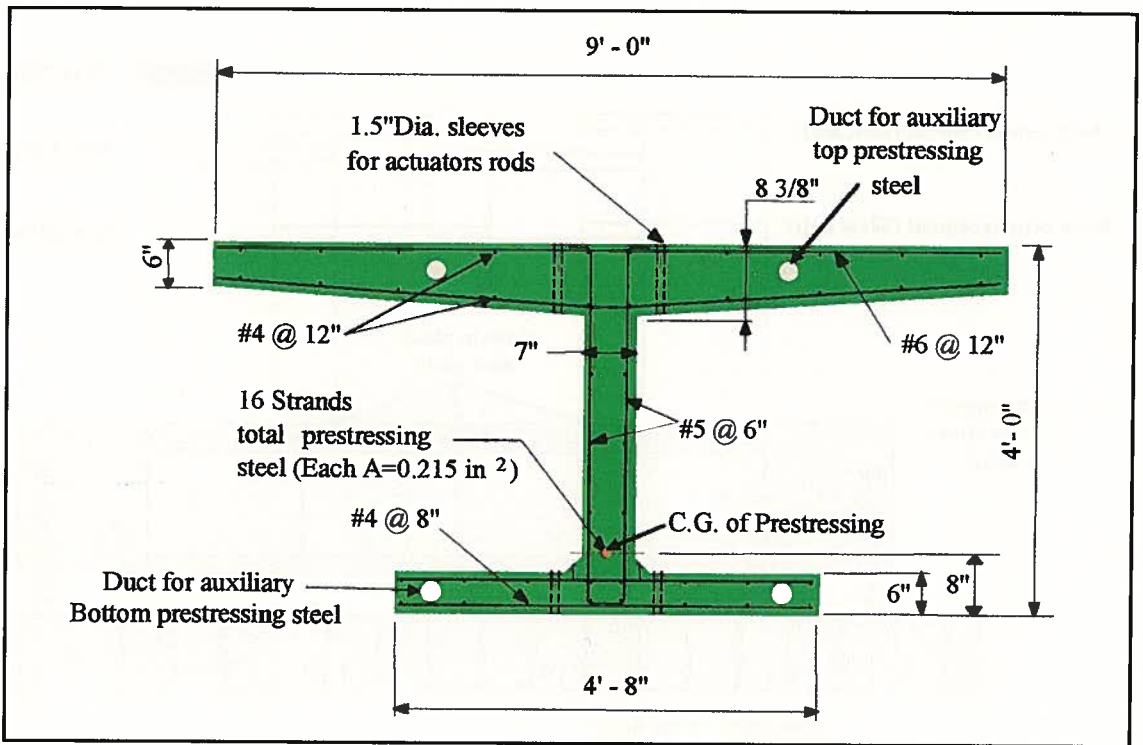


Fig. 3. Cross section of test units.

ply supported at its ends. The test zone had a total length of 24 ft (7.32 m), which represented the center one-third portion of the prototype span. This test zone consisted of four 6 ft (1.83 m) long by 4 ft (1.22 m) deep precast segments (Segments 2 to 5 in Fig. 2). Each test unit was supported at its ends through precast end segments (Segments 1 and 6 in Fig. 2).

Fig. 3 shows the cross section and reinforcement of precast Segments 2 through 5 (see Fig. 2). Half of the prototype box girder section was modeled and idealized in the shape of an equivalent I-section to simplify the test setup.

The variable investigated in this experimental program (Phase I-A) was the presence of mild steel reinforcement crossing the segment-to-segment joints. Test Unit 100INT used 100 per-

cent internal post-tensioning (bonded tendon) with no cast-in-place deck closure joints, or in other words with no mild steel reinforcement crossing the segment joints.

The segments of Unit 100INT were connected by Sikadur 31, SBA (Segmental Bridge Adhesive) slow-set epoxy, which was applied to the entire cross section of the segment-to-segment joints. Specifications of the epoxy are given in Table 2, in which  $\sigma_{comp}$  and  $\sigma_{bond}$  are the compressive and bond strengths, respectively.

Test Unit 100INTCIP used 100 percent internal post-tensioning (bonded tendon) and reinforced cast-in-place deck closures at locations of Joints J2, J3 and J4 (see Fig. 2). Details of the reinforced cast-in-place deck closure joints of Test Unit 100INTCIP were similar to those used in the design of

the new East Span Skyway of the San Francisco-Oakland Bay Bridge.

Two different reinforcement details were incorporated in Unit 100INTCIP at the cast-in-place deck joints. Bent hairpin bars were used on one-half of the cross section and bars with mechanical anchors (welded heads) at their ends were used in the second half (see Fig. 4). Both reinforcement details provide adequate anchorage of the reinforcing bars in the cast-in-place deck joints so their full yield strength can be mobilized. The objective was to study the effect of each of these details on the performance of the joints.

The remaining portions of the joints in Unit 100INTCIP, along the web and bottom slab, were connected by the slow-set segmental bridge adhesive (epoxy). An alternative to the use of

Table 2. Material properties.

Test unit	$f'_c$ (on day of testing) ksi (MPa)				$f_y$ (cast-in-place deck reinforcement) ksi (MPa)		Epoxy properties* (Sikadur 31, SBA) ksi (MPa)	
	Segment No. 1 & 5	Segment No. 3	Segment No. 2, 4 & 6	Cast-in-place deck	Headed bars	Bent bars	$\sigma_{comp}$ (3 days)	$\sigma_{bond}$ (14 days)
100INT	5.11 (35.2)	7.21 (49.7)	6.96 (48.0)	—	—	—	2.0 (13.8)	1.0 (6.9)
100INTCIP	7.25 (50.0)	7.25 (50.0)	5.74 (39.6)	5.87 (40.5)	67.7 (467)	75.6 (521)	2.0 (13.8)	1.0 (6.9)

\* Epoxy properties are those specified by the manufacturer (slow-set epoxy).

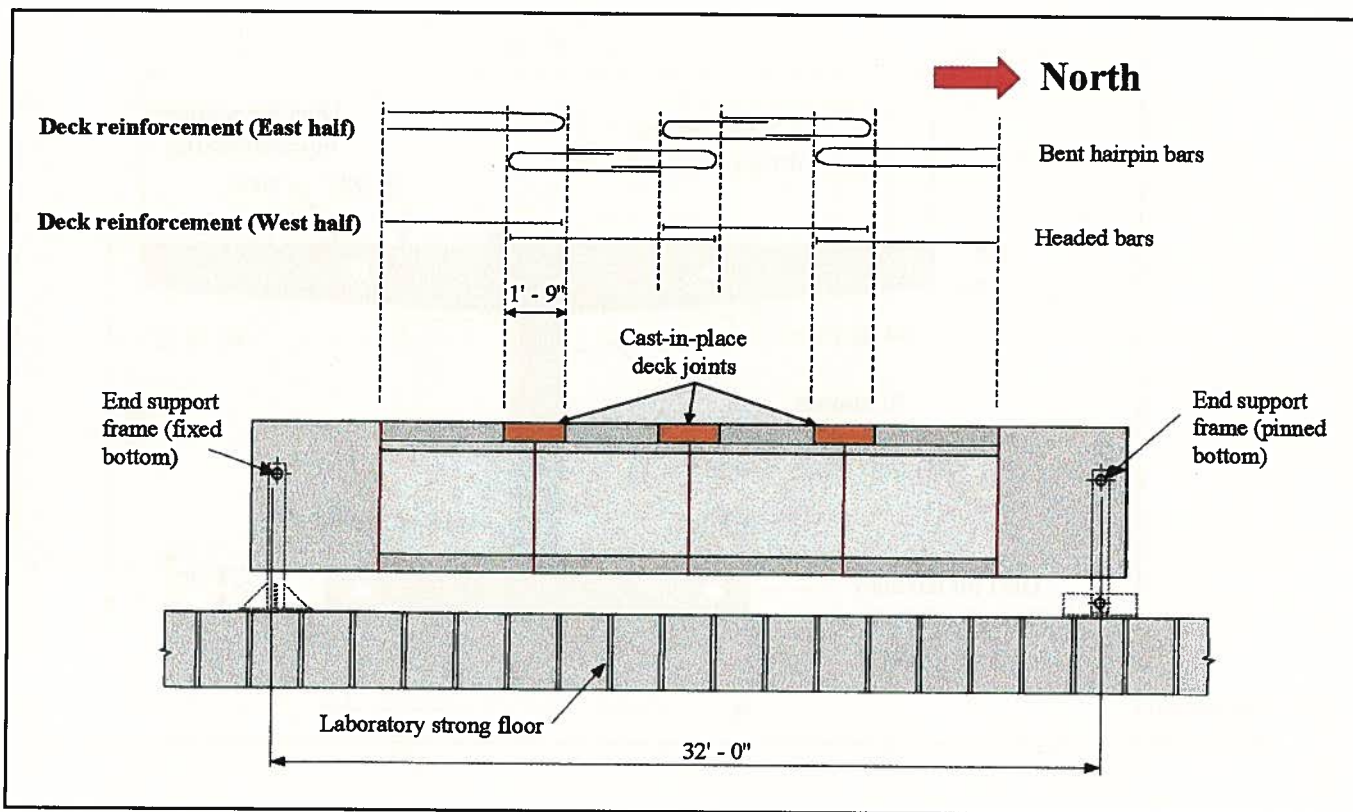


Fig. 4. Reinforced cast-in-place deck joints of Test Unit 100INTCIP.

reinforced cast-in-place deck closure joints in Unit 100INTCIP was to post-tension the deck; however, post-tensioning of the deck was not in the scope of this experimental program.

Each test unit was post-tensioned with 16 strands each of 0.6 in. (15.2 mm) diameter with an ultimate tensile strength of 270 ksi (1860 MPa). The

magnitude of the prestressing force, which is equal for all test units, was calculated so that the concrete stresses resulting from post-tensioning are the same as for the prototype structure. Except for the cast-in-place deck reinforcement in Test Unit 100INTCIP, the layout of the reinforcing bars (Grade 60) is the same for the two test units.

Table 2 gives the measured material properties of concrete and the reinforcement of the cast-in-place deck joint (Test Unit 100INTCIP). In Table 2,  $f'_c$  is the concrete compressive strength on the day of testing of both units and  $f_y$  is the yield strength of the mild steel reinforcing bars crossing the segment-to-segment joints in Unit 100INTCIP.



Fig. 5. A precast segment from Test Unit 100INT.

### Construction of Test Units

As mentioned above, each test unit consisted of six precast segments. Segments 1, 3 and 5 (see Fig. 2) were cast at the same time. This was followed by construction of Segments 2, 4 and 6, which were match-cast against Segments 1, 3 and 5. A bond breaker was applied along the match-cast surfaces so that the segments could be separated after concrete hardening. Fig. 5 shows a precast segment from Unit 100INT with shear keys along the web and alignment keys in the deck and bottom slabs.

The segments of each test unit were assembled on a wooden platform at the UCSD Structures Laboratory. The epoxy was applied to the joint surface

as shown in Fig. 6. After application of the epoxy and placement of each segment in its final position, the test unit was temporarily post-tensioned by four 1 in. (25.4 mm) diameter high strength ASTM A 722 prestressing steel bars (two bars in the top slab and two bars in the bottom slab). The temporary prestressing forces in the high strength bars were determined such that the entire segment-to-segment joint surfaces would have a minimum compressive stress of 40 psi.<sup>5</sup>

It should be remembered that after joining the segments of Unit 100INT-CIP, there was a gap in the deck at the location of Joints J2 to J4 (see Figs. 2 and 4), which was closed later by a cast-in-place concrete slab strip. After joining of the precast segments and closure of the cast-in-place deck joints (Unit 100INTCIP), each test unit was post-tensioned with a jacking force of 720 kips (3203 kN). The effective prestressing force at the time of testing was estimated to be about 600 kips (2669 kN).

The difference between the jacking and effective prestressing forces is due to losses from anchor set, elastic shortening, creep and shrinkage of the concrete as well as relaxation of the prestressing steel. Fig. 7 shows Test Unit 100INT during the post-tensioning operation, which was followed by grouting of the prestressing duct. Fig. 7 also shows the high strength bars used in temporary prestressing of the test units.

The temporary prestressing force in the bottom slab was released after permanent post-tensioning of the test unit, whereas the temporary prestressing force in the top slab was released after vertical loading of the test unit to simulate the prototype dead load stresses. The stressing and loading sequence was designed to avoid cracking of the units before the test. After permanent post-tensioning, the wooden platform supporting the segments during assembly was removed and the test unit was mounted on the two end supports.

### Test Setup

Fig. 8 shows the test unit and the load frame. Each test unit was simply supported by a steel pin and steel links



Fig. 6. Application of epoxy to the joint surface.

at its ends. At one end, the steel links were fixed at their bottom ends to restrain horizontal movement of the test units. At the other end, the steel links were pinned at the bottom (rocker links) to allow rotation of the frame legs and horizontal movement of the test units. The loads were transferred from the test units to the steel links by means of steel pins inside horizontal steel pipes cast into the end segments at the neutral axis of the test units, allowing the ends of the test units to rotate freely.

Four vertical servo-controlled hydraulic actuators were used to apply

external loads to each test unit to simulate the effect of highway loading and vertical seismic displacements on the superstructure. As in the midspan joint of the prototype span, the midspan joint of each test unit was subjected to zero shearing force and the highest bending moment.

At the beginning of the test, each unit was loaded in the downward direction to a prescribed level so that the stresses in the midspan joint were similar to the stresses in the prototype structure under combined dead load, superimposed dead load, as well as prestressing primary and secondary ef-

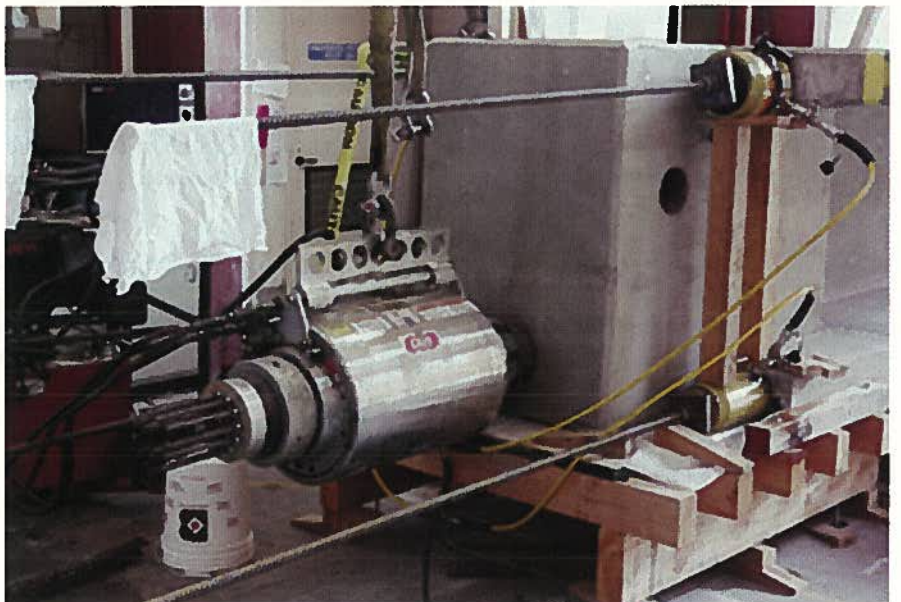


Fig. 7. Post-tensioning of test units.

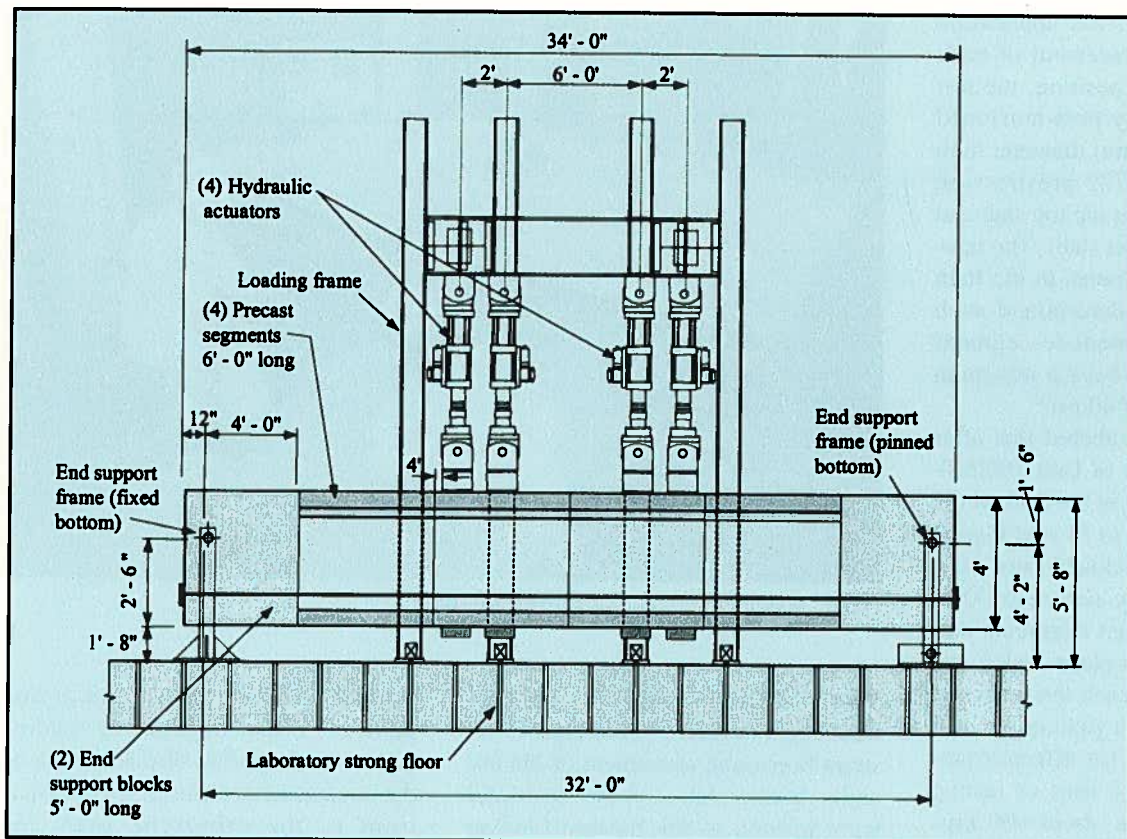


Fig. 8. Test setup.

facts. This load level will be referred to as the reference load level throughout this paper. Each test was conducted as follows:

• **Stage I (Service Load Condition- ing)** — Only the two interior actuators were used in load control during this test stage. Each test unit was loaded to the reference load level at  $P = 74.5$  kips (331 kN), where  $P$  is the load per each actuator. The temporary prestressing force in the top slab was released at this stage.

This was followed by cycling the load  $P$  between 112 and 65 kips (498 and 289 kN) 100,000 times. The purpose of this test stage was to study the

performance of joints under repeated maximum service load cycles.

The upper and lower load limits were calculated so that the stresses in the test units at midspan would be similar to the stresses at midspan for the prototype structure under maximum and minimum service loads. Table 3 gives the estimated concrete stresses at midspan for Units 100INT and 100INTCIP during Test Stage I as well as the corresponding prototype concrete stresses.

• **Stage II (Seismic Test)** — The four actuators were used in displacement control and the forces in the actuators were maintained equal

throughout this test stage. Each test unit was loaded to the reference load level with  $P = 40.5$  kips (180 kN). The test unit was then subjected to fully reversed cyclic displacement at midspan with increasing amplitude to failure.

Three cycles were completed at each displacement level up to 4 in. (102 mm) displacements. Beyond the 4 in. (102 mm) displacement, only one cycle was performed at each displacement level. The applied displacement history during Test Stage II is shown in Fig. 9.

Electrical resistance gauges were used to measure strains in the concrete and prestressing steel. Vertical dis-

Table 3. Concrete stresses in the prototype structure and in test units during Test Stage I.

Load case	P kips (kN)	Concrete stresses,* psi (MPa)					
		Test Unit 100INT		Test Unit 100INTCIP		Prototype structure	
		Top	Bottom	Top	Bottom	Top	Bottom
DL + PT + $M_p''$	74.5 (331)	-473 (-3.26)	-412 (-2.84)	-462 (-3.19)	-407 (-2.81)	-475 (-3.28)	-411 (-2.83)
DL + PT + $M_p''$ + LL + T	112 (498)	-710 (-4.90)	-1.4 (-0.01)	-699 (-4.82)	+4 (0.03)	-1058 (-7.30)	-0.2 (=0)
DL + PT + $M_p''$ - LL	65 (289)	-413 (-2.85)	-516 (-3.56)	-402 (-2.77)	-511 (-3.52)	-413 (-2.85)	-520 (-3.59)

DL = Dead Load; PT = Prestressing primary moments;  $M_p''$  = Prestressing secondary moments;

LL = Live Load; T = Temperature gradient

\* Positive sign indicates tensile stresses.

placements along the span, joint openings at various locations, vertical sliding between the precast concrete segments at each joint and support displacements were measured by means of linear potentiometers.

## EXPERIMENTAL RESULTS

The major experimental results are presented in this section. These experimental results include crack patterns, modes of failure, load-displacement response, performance of joints, strains in prestressing steel, cracking strength and flexural moment capacity.

### Crack Patterns and Modes of Failure

Table 3 indicates that both test units were subjected to very low tensile stresses at the midspan joint during Test Stage I (Service Load Conditioning). Thus, no cracks or joint openings were observed in both test units during Test Stage I. Because of this linear elastic behavior of both test units during Test Stage I, only the results of Test Stage II will be discussed here.

**Test Unit 100INT** — The first crack occurred during downward loading at the midspan joint (Joint J3, Fig. 2) during the first displacement cycle to 0.25 in. (6.35 mm) amplitude (see Fig. 9). The opening of Joint J4 (see Fig. 2) also occurred during the same displacement cycle.

Shear cracks occurred in the web during the same displacement cycle, between the supported ends of the test unit and the load application points (shearing force is approximately zero at the midspan joint). Joint J2 (see Fig. 2) opened during application of the downward displacement to 0.5 in. (12.7 mm) amplitude. Thus, the three interior Joints J2, J3 and J4 (see Fig. 2) opened during loading in the downward direction.

Few additional flexural cracks occurred inside Segments 3 and 4 (see Fig. 2) during subsequent downward loading; however, the widths of these cracks were very small and inelastic deformations of the test unit were concentrated mainly at the midspan Joint J3. New shear cracks developed and

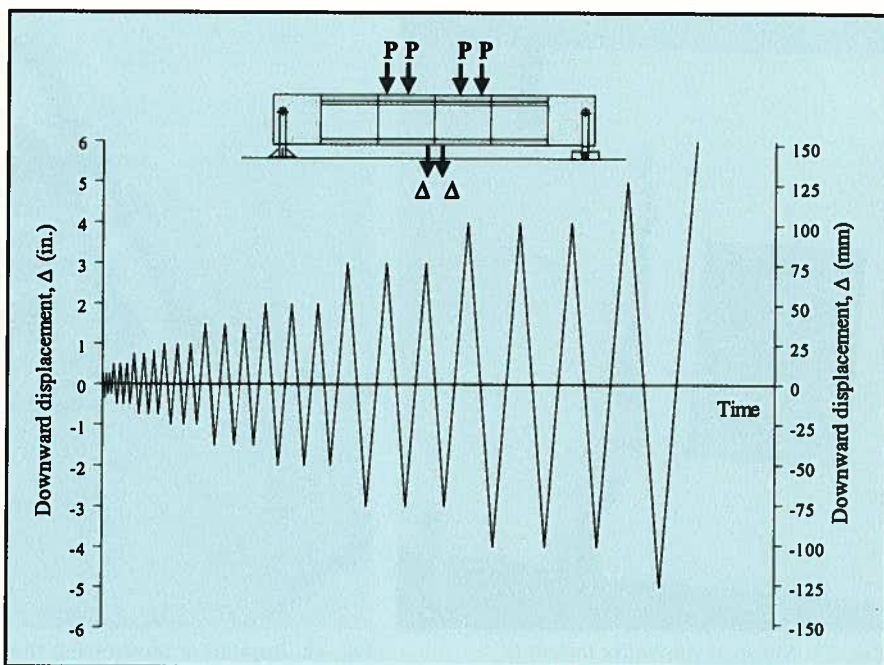


Fig. 9. Loading protocol of Test Stage II.

existing shear cracks propagated during subsequent displacement cycles. Shear cracks crossed the epoxy-bonded joints with no vertical sliding between adjacent precast segments.

The midspan Joint J3 was the only joint that opened during upward loading of Unit 100INT. Joint J3 opened during the 0.5 in. (12.7 mm) displacement cycle. Because Unit 100INT did not have any mild steel reinforcement crossing the joints, the opening of midspan Joint J3 increased significantly under upward loading during subsequent displacement cycles. Fig. 10 shows the midspan joint during the last displacement cycle in the upward loading direction before failure of Test Unit 100INT.

Under downward loading, the midspan Joint J3 opened significantly with increased applied displacement until rupture of the prestressing strands at the midspan joint at a displacement of about 4.8 in. (122 mm) and a total load of 490 kips (2180 kN). Fig. 11 shows the midspan joint after failure of Test Unit 100INT. Fig. 12 shows a closeup view of the ruptured strands.

**Test Unit 100INTCIP** — Development of the crack pattern during downward loading of Test Unit 100INTCIP was similar to the one described above for Unit 100INT. The

first flexural crack occurred at midspan Joint J3 during the 0.25 in. (6.35 mm) displacement cycle. Diagonal shear cracks also occurred during the same displacement cycle. Joints J2 and J4 (see Fig. 2) opened during the 0.50 in. (12.7 mm) downward displacement cycle.

The first flexural crack, in the upward loading direction of Unit

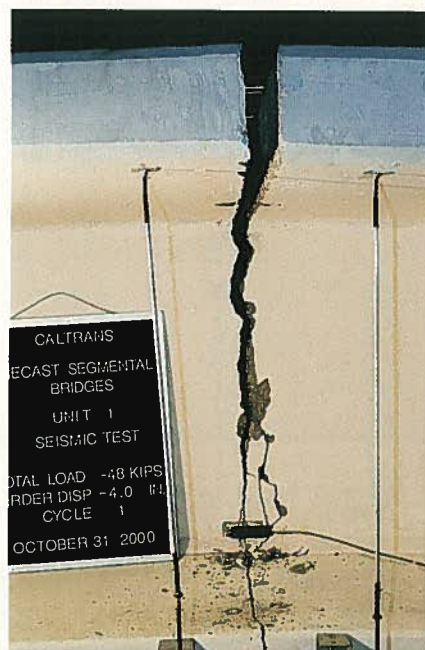


Fig. 10. Midspan joint at maximum upward displacement before failure of Test Unit 100INT.



Fig. 11. Midspan joint after failure of Test Unit 100INT.

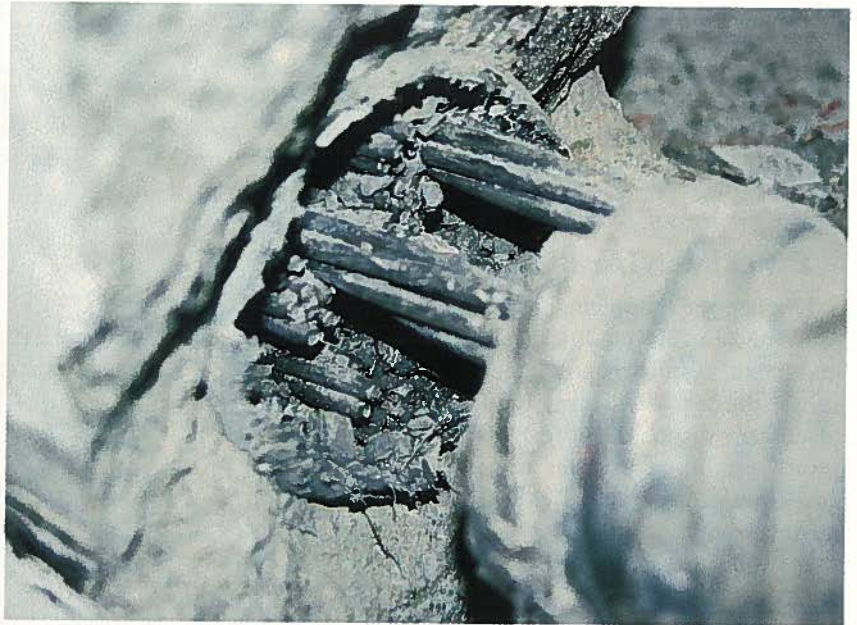


Fig. 12. Rupture of prestressing strands of Test Unit 100INT.

100INTCIP, occurred at the midspan Joint J3 during the 0.75 in. (19.1 mm) displacement cycle. The first crack occurred at the interface between the precast concrete and cast-in-place deck closure joint, rather than at the center of Joint J3.

Additional flexural cracks occurred in the deck under upward loading during subsequent displacement cycles. Because of the continuous deck reinforcing bars in Unit 100INTCIP, several closely spaced and relatively nar-

row cracks occurred in the deck under upward loading, rather than the single wide crack at the midspan joint of Unit 100INT.

Fig. 13 shows the midspan joint at the last displacement cycle in the upward loading direction before failure of Test Unit 100INTCIP. The figure shows the major crack which occurred at the interface between the precast concrete and the deck closure joint; this crack propagated in the web at an angle towards the bottom soffit of the

test unit to join the crack which occurred at midspan under downward loading. The midspan joint opening increased significantly under increasing downward displacements.

Reversed cyclic loading of the deck reinforcement, across the midspan joint, resulted in longitudinal cracks in the cast-in-place concrete, which was followed by buckling of the cast-in-place deck reinforcing bars at a downward displacement of about 3 in. (76.2 mm).

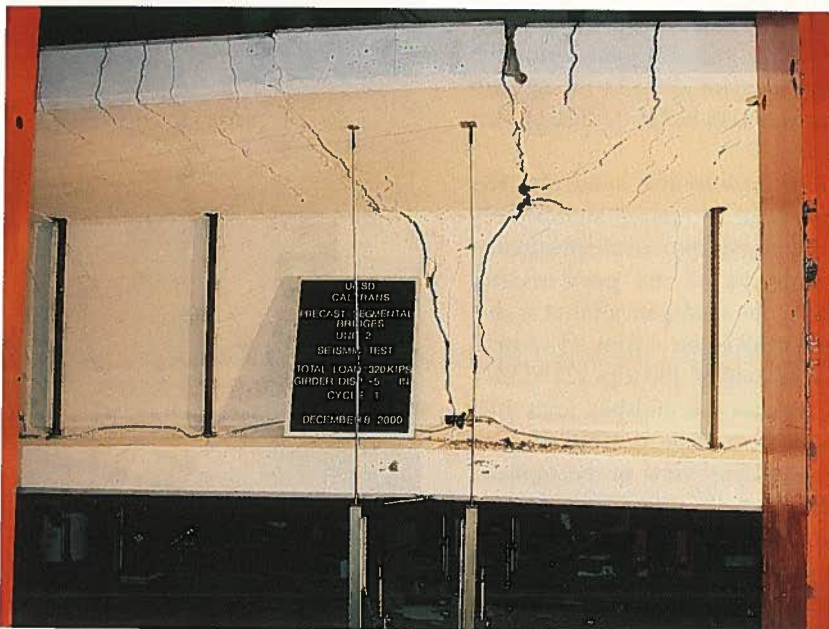


Fig. 13. Midspan joint at maximum upward displacement before failure of Test Unit 100INTCIP.



Fig. 14. Compression failure at midspan joint of Test Unit 100INTCIP.

Table 4. Summary of experimental results.

Test unit	$P_{cr}$ down kips (kN)			$P_{cr}$ up kips (kN)	Peak total load, $P_u$ kips (kN)	
	Joint J2	Joint J3 (midspan)	Joint J4	Joint J3 (midspan)	Maximum*	Minimum
100INT	375 (1668)	307 (1366)	307 (1366)	-93 (-414)	490 (2180)	-93 (-414)
100INTCIP	347 (1544)	324 (1441)	361 (1606)	-103 (-458)	480 (2135)	-327 (-1455)
Test unit	$\Delta_{cr}$ Down in. (mm)			$\Delta_{cr}$ Up in. (mm)	Peak displacement, $\Delta_u$ in. (mm)	
	Joint J2	Joint J3 (midspan)	Joint J4	Joint J3 (midspan)	Maximum*	Minimum
100INT	0.53 (13.5)	0.30 (7.62)	0.30 (7.62)	-0.04 (-1.02)	4.80 (122)	-4.03 (-102)
100INTCIP	0.40 (10.2)	0.25 (6.35)	0.50 (12.7)	-0.05 (-1.27)	5.85 (149)	-4.61 (-117)

Positive sign is for downward load and displacement.

\* Maximum total load or vertical displacement at 6 in. (152 mm) from midspan before failure.

With the concrete severely weakened by reversed cyclic loading, the bars experienced significant buckling and pushed the cover concrete away, which resulted in reduction of the compression area and capacity of the deck. Buckling of the deck reinforcing bars continued until compression failure of the deck at a downward displacement of about 5.85 in. (149 mm); the peak total load of Unit 100INTCIP was 480 kips (2135 kN). Fig. 14 shows the midspan joint and buckling of the deck reinforcing bars after failure of Test Unit 100INTCIP. It is believed that Unit 100INTCIP could have sustained further loading if buckling of the reinforcing bars was prevented; this could have been achieved by providing closed stirrups around the deck top and bottom reinforcement.

Table 4 summarizes the experimental loads and displacements of both test units. In Table 4,  $P_{cr}$  and  $P_u$  are, respectively, the total applied load at onset of joint opening and the maximum total load reached before failure. The vertical displacement at onset of joint opening and the maximum displacement measured at 6 in. (152 mm) from midspan are  $\Delta_{cr}$  and  $\Delta_u$ , respectively.

### Load-Displacement Response

Figs. 15a and 15b show the history of total applied load versus vertical displacement measured at 6 in. (152 mm) from midspan of Test Units 100INT and 100INTCIP, respectively. The sign convention in Fig. 15 is positive for downward loading and dis-

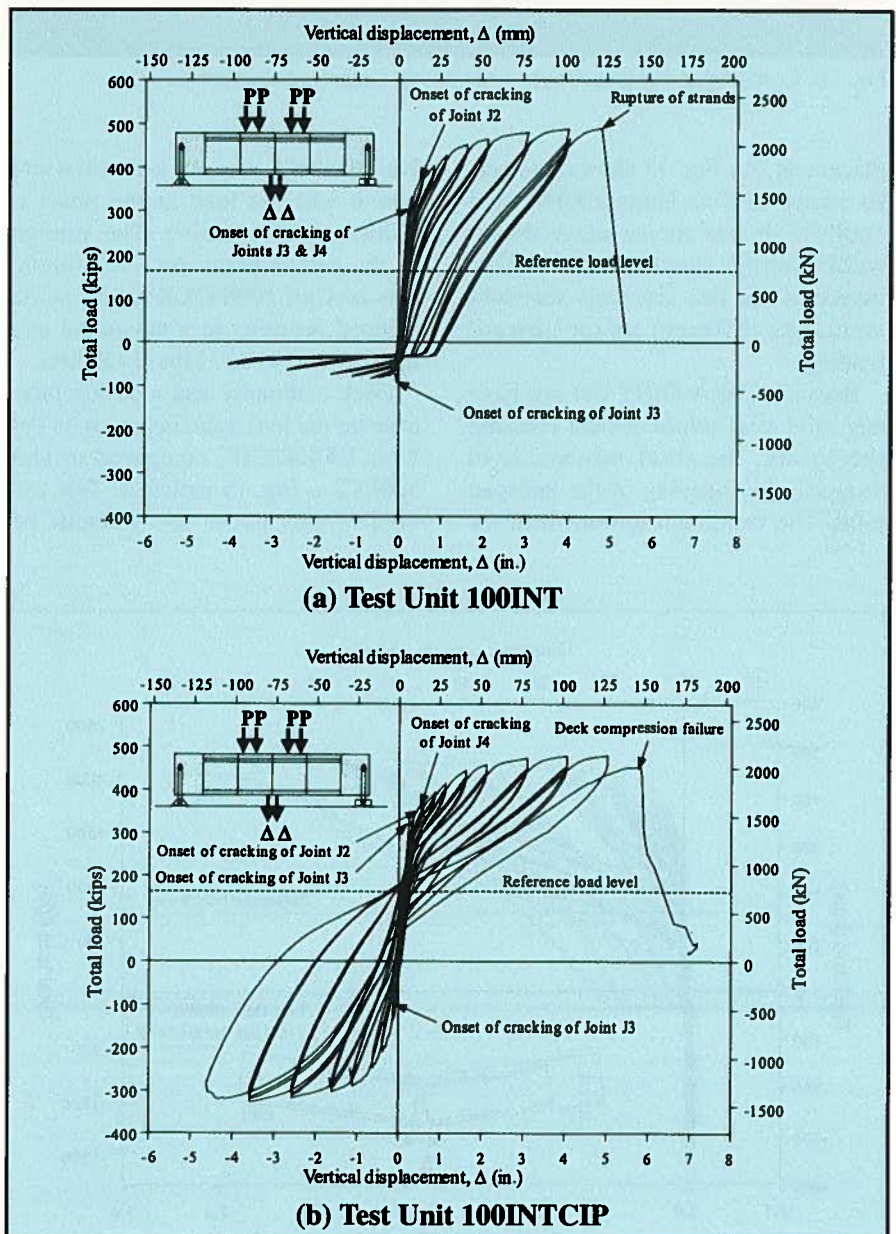


Fig. 15. History of the total load versus vertical displacement measured at 6 in. (152 mm) from midspan of the test units: (a) Test Unit 100INT; and (b) Test Unit 100INTCIP.

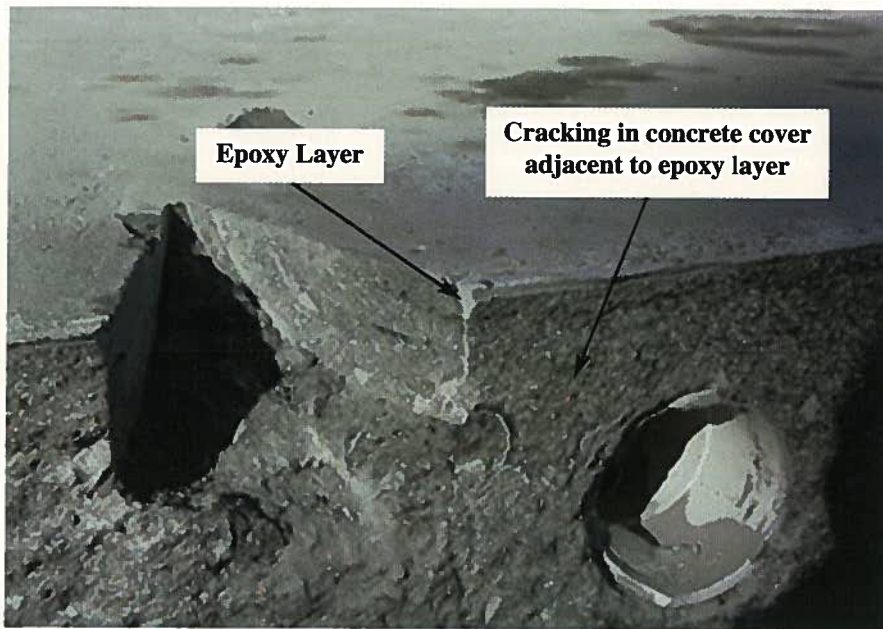


Fig. 16. Cracking of concrete cover adjacent to a segment-to-segment joint.

placement. As Fig. 15 shows, the performance of Test Units 100INT and 100INTCIP was similar under downward loading. However, the performance of the two test units was substantially different under upward loading.

Because Unit 100INT did not have any mild steel reinforcement crossing the joints, the total upward load dropped after opening of the midspan joint. The maximum upward load for

Unit 100INT was 93 kips (414 kN) which was the load at the onset of midspan joint opening. The strength of the cast-in-place deck reinforcing bars of Unit 100INTCIP could be developed resulting in a maximum total upward load of 327 kips (1455 kN).

Deck continuity had a strong influence on the hysteretic behavior of Test Unit 100INTCIP, compared to Unit 100INT as Fig. 15 indicates. Test Unit 100INT had almost no hysteretic be-

havior in the upward loading direction which indicates very low energy dissipation capability. Unit 100INTCIP had better hysteretic behavior under upward loading because of yielding of the continuous deck reinforcement.

The energy dissipated during the complete loading cycle at 3 in. (76.2 mm) displacement was calculated for both test units from the hysteresis loops shown in Fig. 15. The energy dissipation capability was quantified by the equivalent viscous damping coefficient as a ratio of critical damping.<sup>6</sup> Damping ratios of Test Units 100INT and 100INTCIP were determined to be 4.21 and 8.75 percent, respectively, which demonstrates the effect of deck continuity on energy dissipation capability.

Another important issue is the permanent displacement after earthquake occurrence. This corresponds to the displacement at a total downward applied load of 162 kips (721 kN), which is the reference load. Permanent vertical displacements were obtained from Fig. 15 at the reference load of 162 kips (721 kN) for both test units after the first half of the 3 in. (76.2 mm) displacement cycle; the obtained values may be considered as the permanent displacements after this vertical cyclic displacement history.

The above-mentioned permanent residual displacements were 1.17 and 0.53 in. (29.7 and 13.5 mm) for Test Units 100INT and 100INTCIP, respectively. These displacement values represent two-thirds of the difference in permanent vertical displacements expected for the prototype structure between two sections at midspan and at one-third of the span; they are only reported here to show the effect of continuous mild steel reinforcement over the joints on reduction of post-earthquake permanent displacements.

### Performance of Joints

As mentioned earlier, Joints J2, J3 and J4 opened during downward loading of Test Units 100INT and 100INTCIP. Under upward loading of Unit 100INT, only J3 opened, whereas Test Unit 100INTCIP had several closely spaced cracks. Cracking of the concrete cover adjacent to the joint

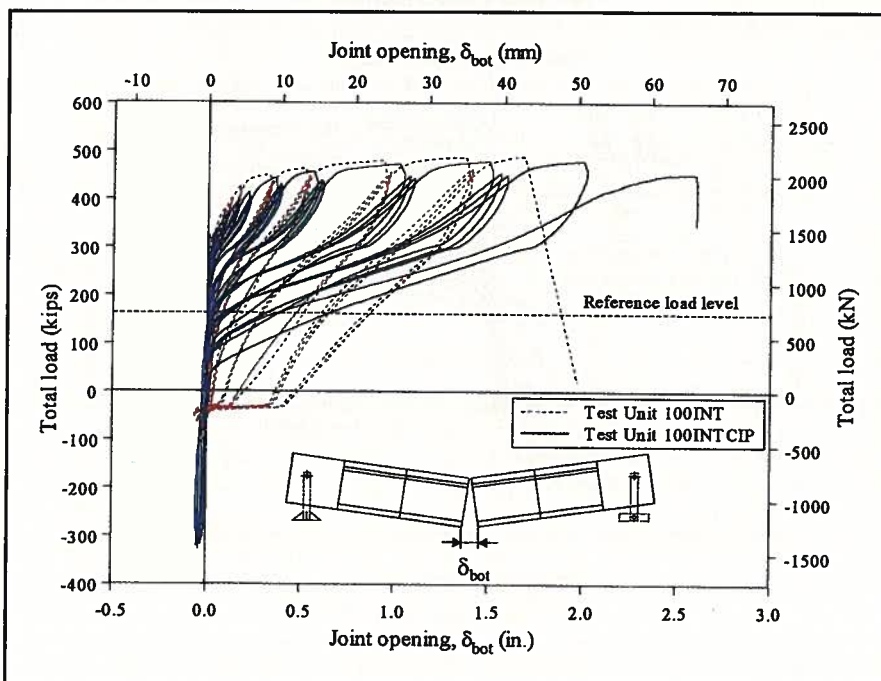


Fig. 17. Opening of midspan joint measured at bottom surface of the test units.

was observed rather than opening of the epoxy joints.

After termination of Test Stage II of Unit 100INT, one segment was cut as shown in Fig. 16 to investigate the opening of the epoxy joint versus cracking of the adjacent concrete cover. Fig. 16 shows the epoxy layer and the failure surface in the adjacent concrete cover. The dominant flexural crack adjacent to the joint occurred through the alignment and shear keys.

As mentioned earlier, the opening of all joints was measured by means of linear potentiometers. Examples of joint opening results are shown in Figs. 17 and 18, which provide the histories of joint opening at midspan measured at the bottom and top surfaces of the test units, respectively. Fig. 17 shows that the joint opening in Unit 100INTCIP was wider than in Unit 100INT. Fig. 17 indicates that permanent joint openings (at reference load level) of Unit 100INTCIP with mild steel reinforcement crossing the joints were less than the permanent joint openings of Unit 100INT.

The effect of deck continuity on joint opening is more pronounced in Fig. 18, which shows the history of joint opening measured at the top surface of Units 100INT and 100INTCIP. Because Unit 100INT did not have any continuous mild steel reinforcement in the deck, the joint opening was significant. Despite its wide opening, the midspan joint of Unit 100INT was closed completely upon unloading during each displacement cycle. Fig. 18 shows the effect of continuous deck reinforcement in controlling the widths of cracks.

Fig. 19 shows the history of bending moment versus midspan joint rotations measured for Test Units 100INT and 100INTCIP. The joint rotation was obtained from the joint openings measured at the top and bottom surfaces of the test units. The maximum rotations of the midspan joint before failure of Test Units 100INT and 100INTCIP were 0.035 and 0.051 radians, respectively.

### Strains in Prestressing Steel

As mentioned earlier, electrical resistance gauges were used to monitor

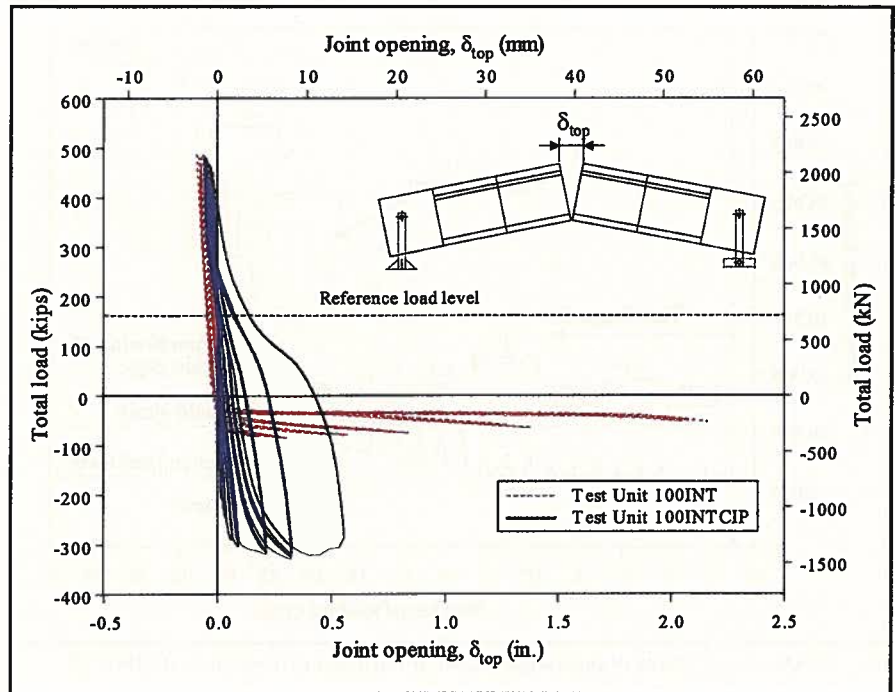


Fig. 18. Opening of midspan joint measured at top surface of the test units.

the strains in the prestressing steel in Test Units 100INT and 100INTCIP. Unfortunately, all the strain gauges mounted on the prestressing steel of Unit 100INT malfunctioned during post-tensioning. Some of the prestressing steel strain gauges malfunctioned during post-tensioning of Test Unit 100INTCIP.

Fig. 20 shows the strain history of one of the surviving strain gauges in

the prestressing steel at midspan of Unit 100INTCIP. The strain is plotted versus the number of loading cycles. In Fig. 20, Cycle 1 represents the time during which the strains were recorded before starting Test Stage II. Fig. 20 also shows the strain in the tendon at midspan of Unit 100INTCIP as obtained from the finite element analysis.

The yield strain level, represented

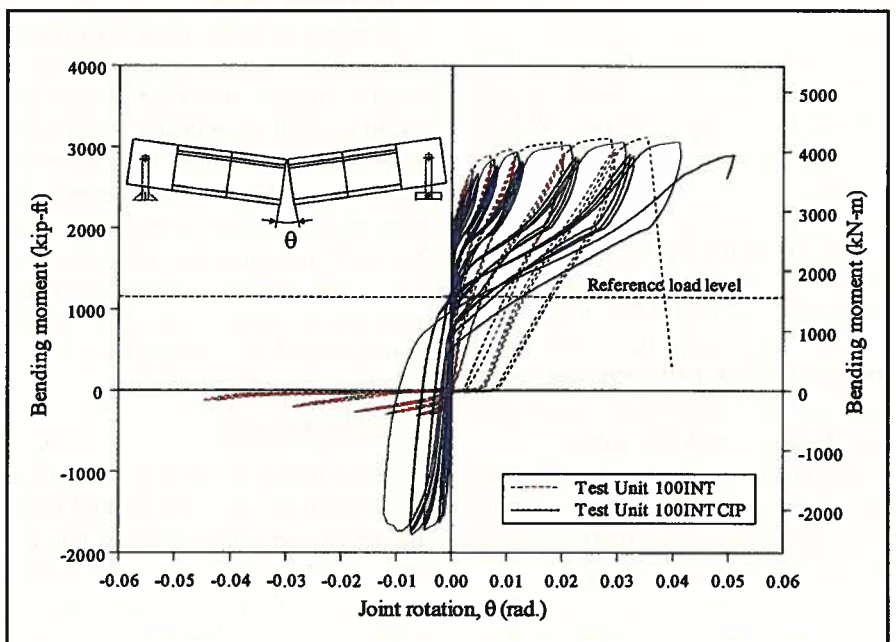


Fig. 19. History of midspan joint rotation versus bending moment.

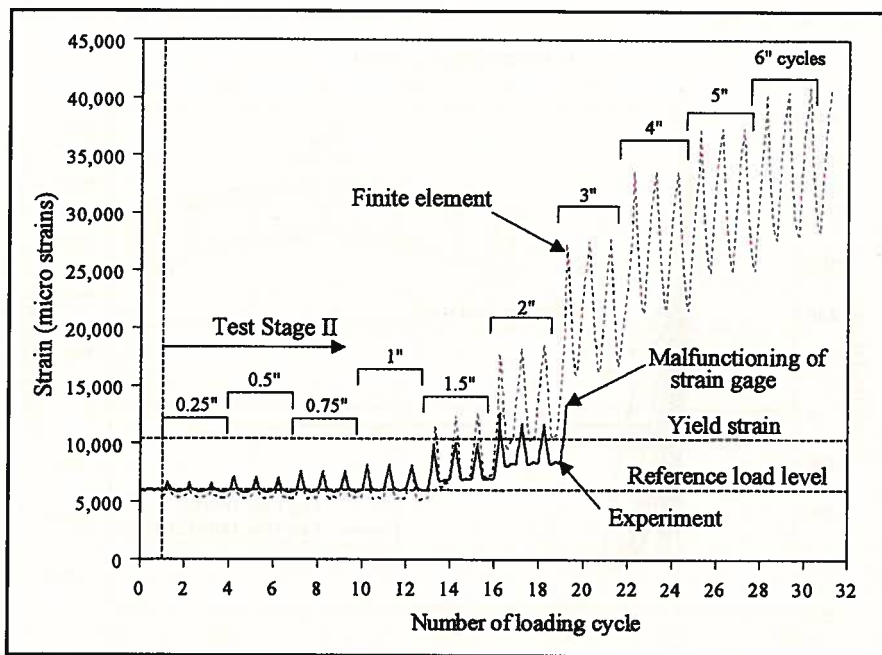


Fig. 20. History of strain in prestressed steel at midspan of Test Unit 100INTCIP.

by a horizontal dashed line in Fig. 20, corresponds to the 0.2 percent offset yield strain definition. The strain in the tendon,  $\epsilon_{ps}$ , measured just before starting Test Stage II was about 5900 micro strains. The corresponding stress,  $f_{ps}$  (ksi), is calculated from the following equation<sup>7</sup> (assuming elastic modulus,  $E_{ps} = 29000$  ksi = 200 GPa):

$$f_{ps} = 29,000 \epsilon_{ps} \left\{ 0.025 + \frac{0.975}{\left[ 1 + (118 \epsilon_{ps})^{10} \right]^{0.1}} \right\} \quad (1)$$

The corresponding stress in the tendon before starting Test Stage II was about 171 ksi (1180 MPa) and the effective prestressing force was about 588 kips (2616 kN). This measured prestress force was close to the calculated 600 kip (2669 kN) force.

The strain in the tendon (see Fig. 20) increased with applied loading until the strain gauge malfunctioned during the first cycle to 3 in. (76.2 mm) displacement (downward loading). The strain recorded before malfunctioning of the strain gauge ex-

ceeded 0.013 and the corresponding stress [Eq. (1)] was about 249 ksi (1717 MPa), or 92 percent of the ultimate tensile stress of the strands. It is believed that the stress in the tendon was very close to the ultimate stress of 270 ksi (1860 MPa) when the deck compression failure occurred.

Fig. 20 indicates that plastic deformations of the tendon occurred beyond the 1.0 in. (25.4 mm) displacement cycles. Also, the strain in prestressing steel increased with downward displacement and reduced at zero displacement.

In response to the upward displacements the strain also increased, but to a smaller degree than from downward loading, and then reduced at zero displacement. The small increase in strains during upward loading was because the prestressing tendon was above the neutral axis, indicating that while the bottom soffit concrete strains were compressive the strains at the level of the prestressing steel were tensile.

### Cracking Strength

The concrete cracking strength at joint locations was determined using the known section properties, the experimental flexural moments at onset of cracking, or joint opening, and the effective prestressing force. The midspan Joint J3 in Unit 100INT

opened under downward loading when the concrete reached a tensile stress of  $3.25\sqrt{f'_c}$  (psi) [=  $0.27\sqrt{f'_c}$  (MPa)]. Joint J3 in Unit 100INTCIP opened at a concrete tensile stress of  $5.61\sqrt{f'_c}$  (psi) [=  $0.47\sqrt{f'_c}$  (MPa)]. It should be mentioned that no tensile stresses are allowed to occur under service loads according to Section 9.2.2.2 of the AASHTO Guide Specification for Design and Construction of Segmental Concrete Bridges.<sup>1</sup>

Cracking of the top surface in Unit 100INTCIP occurred at a concrete tensile stress of about  $4.00\sqrt{f'_c}$  (psi) [=  $0.33\sqrt{f'_c}$  (MPa)], which was relatively low considering the continuity of the deck. The onset of cracking occurred in the deck at the interface between the precast concrete and that of the cast-in-place deck closure joint. The relatively weak interface between the precast and cast-in-place concretes resulted in this relatively low cracking strength.

### Flexural Moment Capacity

The calculated ultimate moment capacities of Test Units 100INT and 100INTCIP were 2993 and 2974 kip-ft (4058 and 4032 kN-m), respectively. The ultimate moment capacities of both units were determined according to the provisions of Article 9.17 of the AASHTO Standard Specifications.<sup>3</sup> The experimental peak flexural moments were 3126 and 3062 kip-ft (4238 and 4151 kN-m) for Units 100INT and 100INTCIP, respectively.

The ratios of experimental to calculated moment capacity were 1.04 and 1.03 for Units 100INT and 100INTCIP, respectively. This indicates that the flexural strength of precast segmental bridge superstructures with internally bonded tendons can be accurately estimated using the equations of the AASHTO Standard Specifications.<sup>3</sup>

### Deck Joint Reinforcement

As mentioned earlier, two different details were used for the reinforcement of the cast-in-place deck joints (see Fig. 4) of Test Unit 100INTCIP. Bent hairpin bars were used on one-half of the cross section whereas bars with mechanical anchors (welded heads) at their ends were used in the second half. Widths of cracks in the

top surface of the deck were measured at several locations in the two halves of the cross section.

No difference was observed in performance of the two cross section halves in terms of crack openings. As mentioned earlier, failure of Unit 100INTCIP was initiated by buckling of deck mild steel reinforcing bars which pushed the concrete cover away and resulted in the deck compression failure.

Buckling of deck reinforcement could have been prevented by use of stirrups that enclose the top and bottom longitudinal bars of the deck. Although there is no difference between headed and bent hairpin bars in terms of structural performance of the joints, use of headed bars would speed up the construction and make it easier especially if stirrups are used to enclose the deck top and bottom reinforcing bars as recommended above.

## FINITE ELEMENT ANALYSIS

Three-dimensional finite element models of the test units were developed. The finite element models and the major finite element results are presented in this section.

### Description of the Finite Element Models

Detailed finite element models were developed for both test units (see Fig. 21). Analyses were conducted using the general-purpose finite element program ABAQUS,<sup>8</sup> interfaced with the ANACAP<sup>9</sup> concrete material model.

The concrete was modeled as 3-D, eight-node, solid brick elements with strain-hardening and strain-softening capabilities in compression, and tension cutoff with cracks that do not close upon closure.<sup>9</sup> Confinement effects were assumed to be negligible and the unconfined concrete strength was taken as 7.5 ksi (51.7 MPa). The model was developed in a similar way to the test units, with no solid elements crossing the joints between the precast segments and no connection between solid elements on either side of the joints.

The joints were free to open by providing double nodes and compression-

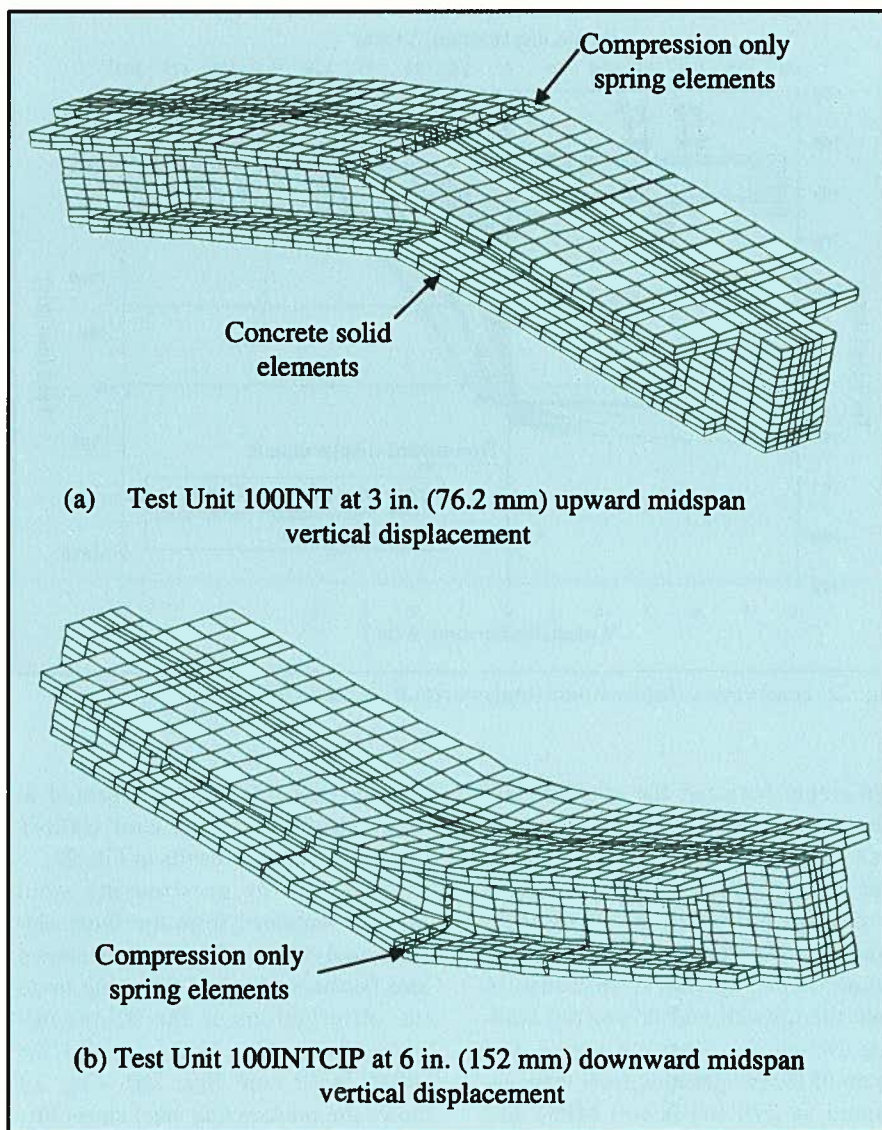


Fig. 21. Finite element models and deformed shapes of the test units: (a) Test Unit 100INT at 3 in. (76.2 mm) upward midspan vertical displacement; and (b) Test Unit 100INTCIP at 6 in. (152 mm) downward midspan vertical displacement.

only springs at all nodes in the cross section at locations of joints. Prestressing steel was modeled by truss elements and connected to the concrete nodes at each 12-in. (305 mm) cross section, representing bonded strands. All mild steel reinforcement was modeled as 1-D sub-elements in the solid concrete elements.

No mild steel reinforcement crossed the joints of Unit 100INT and thus they served only to prevent failure within the precast segments and had no impact on the overall load-displacement response of the structure. Test Unit 100INTCIP with the cast-in-place deck joint, required mild steel reinforcing bars to be placed across the joints at the deck level; these mild

steel bars were activated and yielded under upward loading of the test unit.

At the joints, the prestressing steel was not connected to the center nodes, but to nodes at sections 12 in. (305 mm) on either side of the centerline. This represented an idealized unbonded length at the joints of 24 in. (610 mm), which was consistent with the assumed plastic hinge length used in designing the test units.<sup>4</sup> Loading was applied to the models in displacement control as shown in Fig. 9.

### Finite Element Results

**Test Unit 100INT** — Analysis results of Unit 100INT are given in Figs. 22 and 23. There was very close

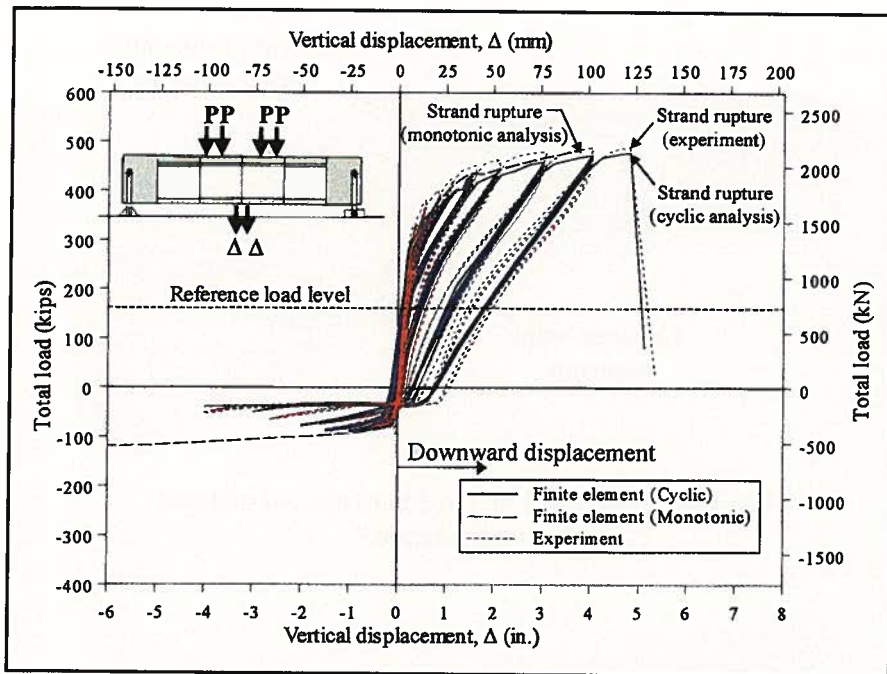


Fig. 22. Load versus displacement analysis results of Test Unit 100INT.

agreement between the analysis and measured load-displacement responses (see Fig. 22). Analysis results showed that the model behaved very similarly to the test unit in terms of ultimate load, displacement at failure, and shape of the hysteretic response in both the upward and downward loading directions. Rupture stress and strain of the prestressing steel were assumed as 270 ksi (1860 MPa) and

0.04, respectively, which appeared to be reasonable based on Unit 100INT load-displacement results in Fig. 22.

Strains of the prestressing steel could be obtained from the finite element analysis but they are not shown here because they had the same trend and observations as the strains obtained from the analysis of Unit 100INTCIP (see Fig. 20). Fig. 23 shows the prestressing steel stress his-

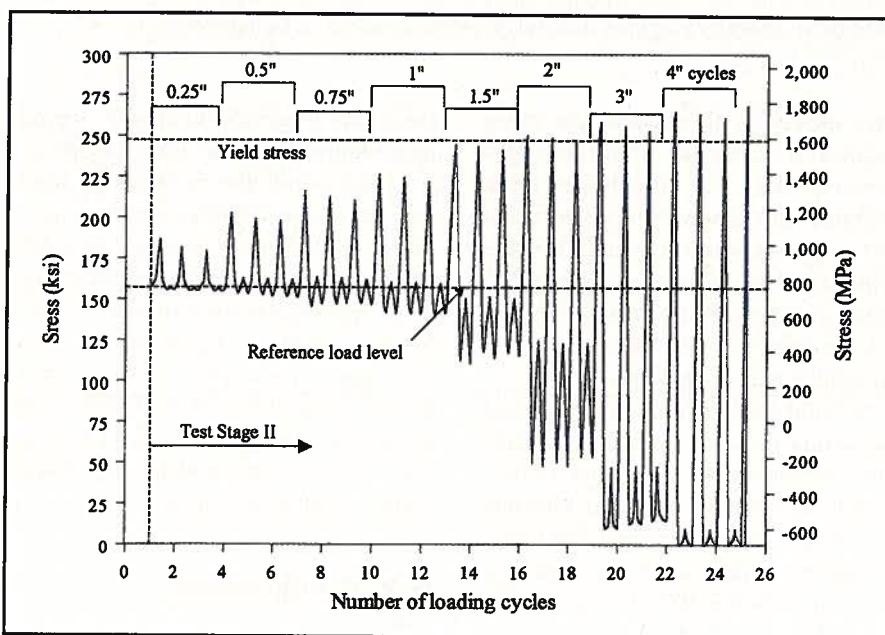


Fig. 23. Stress history analysis results of prestressing steel at midspan of Test Unit 100INT.

tory (stress versus loading cycle number) at midspan (Joint J3, see Fig. 2) from the analysis of Test Unit 100INT. Plastic deformations of the tendon occurred beyond the 1 in. (25.4 mm) displacement cycle. Of interest with the permanent plastic deformations is that with increasing, unrecoverable, strains, the initial prestress force was lost (see Fig. 23).

It is clear from Fig. 23 that beyond 1 in. (25.4 mm) displacement, the initial prestress force started to reduce significantly, and was completely lost (at zero displacement, or at the reference load level) following 4 in. (102 mm) of downward displacement. This may have important consequences in the design of precast concrete structures, where under a severe earthquake the prestressing force is diminished or lost altogether before rupture of the strand.

**Test Unit 100INTCIP** — Samples of analysis results of Test Unit 100INTCIP are given in Figs. 20 and 24. Although the shape of the monotonic load-displacement results for the upward and downward loading directions matched the test results very well, the cyclic analysis results did not follow as closely. Failure from both monotonic and cyclic analyses was from rupture of the prestressing steel, whereas the observed collapse during the experiment was from compression failure of the deck at the midspan cast-in-place joint.

As mentioned earlier, buckling of the cast-in-place deck reinforcement initiated the deck compression failure of Unit 100INTCIP. The analysis model was not able to catch this type of failure because the cast-in-place deck steel was modeled by 1-D truss elements, which do not have the ability to buckle. It may be of interest to model the cast-in-place deck steel with beam elements to allow buckling of the reinforcement.

Although the mode of failure was different than observed, the force and displacement at failure from the cyclic analysis matched the measured results very closely. Note that the monotonic analysis showed rupture of the prestressing steel at a much earlier displacement, demonstrating that the analysis model was able to spread the

strain penetration out further with increased number of cycles, due to cracking and damage of the elements in the vicinity of the prestressing steel.

It is not clear at this point why the unloading stiffness was different during load reversal (may be due to the assumed prestressing steel model) and why, in the upward loading direction, the force at increasing peak displacements reduced and diverged from the test results and those of the monotonic analysis. The results from monotonic analyses clearly demonstrate that the basic model was correct.

Strain history results are provided in Fig. 20. One strain gauge on the prestressing steel at the midspan joint remained intact to the first cycle to 3 in. (76.2 mm), allowing comparisons to the cyclic strain analysis results at least to 2 in. (50.8 mm) of downward and upward displacement. The experimental and finite element variations of the strain with increased loading had the same trend as Fig. 20 indicates.

## DESIGN IMPLICATIONS

This paper presents the experimental and analytical results of the test units with internally bonded tendons only. Definitive recommendations for seismic design of precast segmental bridge structures can only be made upon completion of the three phases of the research project. However, based on the results presented in this paper, the following can be implied for seismic design of precast segmental bridge superstructures post-tensioned with internally bonded tendons:

- Opening of the epoxy-bonded joints, or cracking at the joint locations, occurs when the concrete reaches a tensile stress of about  $3\sqrt{f'_c}$  (psi) [ $= 0.25\sqrt{f'_c}$  (MPa)]. Cracking of the deck with cast-in-place closure joints occurs at a relatively low concrete tensile stress of about  $4\sqrt{f'_c}$  (psi) [ $= 0.33\sqrt{f'_c}$  (MPa)].

- The flexural capacity of precast segmental bridge superstructures can be accurately predicted using the provisions of Article 9.17 of the AASHTO Standard Specifications.<sup>3</sup>

- Finite element analyses showed that the effective prestressing force reduces after earthquake occurrence, es-

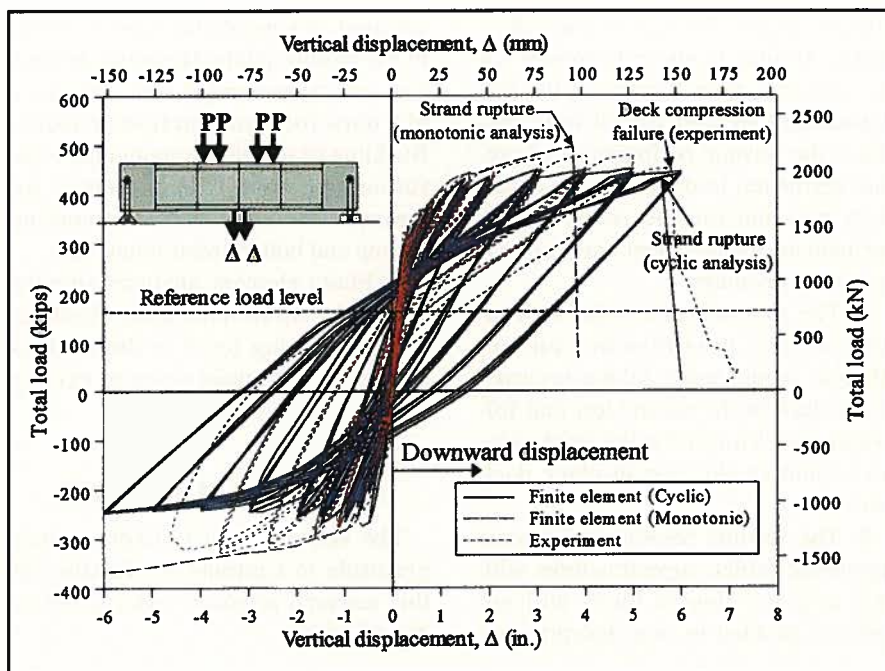


Fig. 24. Load versus displacement analysis results of Test Unit 100INTCIP.

pecially if the superstructure segment-to-segment joints are subjected to significant joint openings or rotations during the earthquake (see Fig. 23). External post-tensioning may be a good alternative in which case less reduction in the effective prestressing force is expected in external tendons.

- To prevent the explosive compression failure of precast concrete superstructures with cast-in-place deck closure joints, the deck top and bottom layers of longitudinal mild steel reinforcement should be enclosed by means of closed stirrups in the cast-in-place closure zone. The same should be done if the ductility of the superstructures needs to be increased.

## CONCLUSIONS

A large-scale experimental program and finite element studies are currently in progress to investigate the seismic performance of segment-to-segment joints of prestressed, precast segmental bridge superstructures. The experimental program and the analytical model calibrations of two test units with internally bonded tendons are presented in this paper. The joints of the first test unit were epoxy bonded with no mild steel reinforcement crossing the joints, whereas the second test unit had reinforced cast-in-place

deck closure joints with the remaining portions of the joints connected by epoxy.

The following conclusions can be drawn:

1. Opening of an epoxy-bonded joint occurs due to cracking of the concrete cover adjacent to the joint rather than opening of the epoxy joint. The concrete cover adjacent to the joint has relatively low cracking strength compared to the concrete of the precast segments. The dominant flexural vertical crack adjacent to the joint occurs through the alignment and shear keys.

2. Crack patterns for both units were similar under downward loading. Because of the mild steel reinforcement crossing the joints, the deck of the second test unit experienced several closely spaced and relatively narrow cracks under upward loading in lieu of one single wide crack at the midspan joint of the first test unit with no mild steel reinforcement crossing the joints.

3. The segment-to-segment joints can experience significant repeated openings and closures under reversed cyclic loading without failure even if there is no mild steel reinforcement crossing the joints. However, permanent deformations and joint openings are reduced if there are mild steel reinforcing bars crossing the segment-to-

segment joints. The cast-in-place deck joints, similar to those proposed for the new East Span Skyway of the San Francisco-Oakland Bay Bridge, enhance the seismic performance of precast segmental bridges in terms of energy dissipation and reduction of permanent displacements and permanent joint openings.

4. The first test unit failed by rupture of the prestressing tendon, whereas compression failure occurred in the deck of the second test unit following buckling of mild steel reinforcement of the cast-in-place deck joint.

5. The seismic response of precast segmental bridge superstructures with cast-in-place closure joints will not differ if headed or bent hairpin bars

are used as longitudinal reinforcement in the closure joints. However, headed bars are recommended over bent hairpin bars for construction reasons. Buckling of the deck longitudinal reinforcement should be prevented by means of closed stirrups that confine the top and bottom reinforcing bars.

6. Finite element analyses showed that under severe earthquake loading, the prestressing force in the tendons could diminish under repeated cycling in the inelastic strain range.

## ACKNOWLEDGMENTS

The authors want to express their gratitude to Caltrans for funding of this research program under Contract No. 59A0051.

Members of the AASHTO-PCI-ASBI technical research committee are acknowledged for participating in the development of this research project.

J. Muller International, San Diego, prepared the construction drawings of the test units.

Sika Corporation donated the epoxy.

Dywidag-Systems International (DSI), USA, donated the post-tensioning strands, high-strength bars and hardware.

Headed Reinforcement Corporation (HRC), California, donated the headed bars.

The authors wish to express their appreciation to the PCI JOURNAL reviewers for their valuable and constructive comments.

## REFERENCES

1. AASHTO, *Guide Specification for Design and Construction of Segmental Concrete Bridges*, Second Edition, American Association of State Highway and Transportation Officials, Washington, DC, 1999.
2. AASHTO-PCI-ASBI, *Segmental Box Girder Standards for Span-by-Span and Balanced Cantilever Construction*, American Association of State Highway and Transportation Officials, Washington, DC, Precast/Prestressed Concrete Institute, Chicago, IL, and American Segmental Bridge Institute, Phoenix, AZ, 1997.
3. AASHTO, *Standard Specifications for Highway Bridges*, 13th Edition, American Association of State Highway and Transportation Officials, Washington, DC, 1983.
4. Dowell, R. K., Silva, P. F., and Seible, F., "Precast Segmental Bridge Performance in Seismic Zones: Phase I, Test Unit Design," Progress Report submitted to Caltrans, April 2000, 30 pp.
5. ASBI, *Recommended Contract Administration Guidelines for Design and Construction of Segmental Concrete Bridges*, American Segmental Bridge Institute, Phoenix, AZ, March 1995, pp. 109-116.
6. Chopra, A. K., *Dynamics of Structures*, Prentice Hall, Inc., Princeton, NJ, 1995, 729 pp.
7. Collins, M. P., and Mitchell, D., *Prestressed Concrete Structures*, Response Publication, Toronto, Canada, 1997.
8. Hibbitt, Karlson, and Sorenson, *ABAQUS User's and Theory Manual*, Version 5.8, 1999.
9. ANATECH Corporation, *ANACAP-U User's and Theory Manual*, Version 2.5, 1997.